Dielectrics for Terahertz Metasurfaces: Material Selection and Fabrication Techniques

Ako, Rajour Tanyi; Upadhyay, Aditi; Withayachumnakul, Withawat; Bhaskaran, Madhu; Sriram, Sharath

Ako, Upadhyay, A., Withayachumnakul, W., Bhaskaran, M., & Sriram, S. (2019). Dielectrics for Terahertz Metasurfaces: Material Selection and Fabrication Techniques. Advanced Optical Materials, 2019(3), 1–16. https://doi.org/10.1002/adom.201900750
Document Version: Accepted Manuscript

Published Version: https://doi.org/10.1002/adom.201900750

Dielectrics for Terahertz Metasurfaces: Material Selection and Fabrication Techniques

Rajour Tanyi Ako,[1]* Aditi Upadhyay,[1] Withawat Withayachumnankul,[2] Madhu Bhaskaran,[1] and Sharath Sriram[1]*

[1] Functional Materials and Microsystems Research Group and the Micro Nano Research Facility, RMIT University, Melbourne, Australia

[2] Terahertz Engineering Laboratory, School of Electrical and Electronic Engineering, The University of Adelaide, Adelaide, SA 5005, Australia

*Corresponding authors email: rajour.tanyi.ako@student.rmit.edu.au, sharath.sriram@rmit.edu.au

Abstract

Manipulation of terahertz radiation opens new opportunities that underpin application areas in communication, security, material sensing, and characterisation. Metasurfaces employed for terahertz manipulation of phase, amplitude, or polarization of terahertz waves have limitations in radiation efficiency which is attributed to losses in the materials constituting the devices. Metallic resonators–based terahertz devices suffer from high ohmic losses, while dielectric substrates and spacers with high relative permittivity and loss tangent also reduce bandwidth and efficiency. To overcome these issues, a proper choice of low loss and low relative permittivity dielectric layers and substrates can improve field confinement and reduce dissipation. Alternatively, replacing metallic resonators with a moderate relative permittivity dielectric material that supports cavity mode resonances also reduces dissipation due to the absence of conduction current. Herein, we provide an overview of dielectric materials employed as spacers and dielectric resonators, and the fabrication methods employed to realize these devices at the terahertz frequency range. Material selection guidelines, material-specific and application-specific fabrication quality metrics are outlined, and new techniques are proposed.

Keywords

dielectric spacers, dielectric resonators, terahertz devices, metasurfaces, low loss, efficiency

Introduction

Application of terahertz radiation spanning 0.1 to 10 THz is paving a new era[1] in a wide range of fields, particularly directed towards faster, high data rate post-5G communication network,[2-4] high resolution imaging,[5-8] stand-off detection,[8-10] and non-contact sensing of materials.[10-12] More so, it is increasingly employed in research for the characterisation of optical properties and screening of biological/chemical compounds based on distinctive spectral signatures resulting from vibrational modes of covalent and hydrogen bonds.[8,13-16] The focus on this spectrally rich region is attributed to the highly coherent and non-ionizing nature of terahertz radiation, wide un-allocated frequency bands, distinctive wavelengths, and their penetration through a significant depth of dielectric materials. Terahertz technology is geared towards realizing devices that can efficiently manipulate the phase, amplitude, and polarization of terahertz radiations for the above-mentioned myriad of applications.

However, progress in this domain is held back by low terahertz power available from compact sources, high free-space path loss, and limited choice of materials that exhibit less absorption of terahertz waves.[17] Owing to the fact that natural materials demonstrate weak wave–matter interaction at terahertz frequencies, terahertz devices with engineered sub-wavelength resonant metallic inclusions on dielectric spacers have been realized, to interact strongly with an incident electromagnetic wave.

In the past, metamaterials have been a promising route to building terahertz devices. These devices have in essence been engineered as three-dimensional (3D) resonating elements that effectively manipulate both permittivity and permeability of an effective medium to couple to free space. The underlining disadvantage of these structures is the difficulty involved in the fabrication of 3D geometrical structures using standard semiconductor fabrication techniques. Standard fabrication techniques are generally amenable to two-dimensional (2D) design with extrusion of these structures into thickness (the third, vertical dimension). Moreover, the choice and availability of dielectric materials and metals that provide sufficient interaction while retaining device efficiency has proved challenging.[13,18-20]

Recently, effective manipulation of electromagnetic wave has been widely demonstrated with 2D metasurfaces, which were originally employed as building blocks for 3D metamaterials. In these lower-dimension designs, effective manipulation of terahertz waves for various applications is achieved by carefully designing sub-wavelength resonant structures as is evident in published review articles.[21,22] Metasurfaces present high degree of compactness that enhances radiation efficiency. Additionally, the planar form-factor of metasurfaces enables their realization with standard microfabrication techniques and can easily be coupled to integrated platforms. Moreover, all-

dielectric metasurfaces are also feasible due to ease of fabrication using a one–step standard microfabrication technique.

A key to efficient electromagnetic manipulation is the choice of material composition of these metasurfaces. Herein, the metallic resonators support conduction current and the dielectric spacers aid energy storage. Strong coupling of these resonators to free space is required for functional free-space devices. However, at high frequencies Drude metals experience high power dissipation associated with finite conductivity, roughness, and skin depth. These impose limitations on the efficiency of these devices.[23] Moreover, strong field confinement around resonators interacts strongly with a supporting dielectric layer. Thus, the importance of using dielectrics with low loss is favored. Polymers have relatively low loss. They can also be easily applied to desired thicknesses using cost-effective spin-on techniques, with an added advantage of flexibility for conformal devices, as opposed to non-flexible silicon dioxide (SiO_2) and quartz substrates that were commonly used. These low relative permittivity materials support wide bandwidth applications.

Alternatively, to enhance radiation efficiency, metallic resonators can be replaced with dielectric resonators of moderate relative permittivity. Due to the absence of conduction current, the loss can be significantly reduced. Despite that, resonators can be made of lossy dielectric materials so to support high energy capture and dissipation. As a hybrid between the two extrema, tunable resonators can be derived from dielectric materials with variable charge carrier densities that can be tuned by light, bias voltage, or heat for dynamic responses to phase, amplitude, or polarization.

This review article first covers different types of dielectric materials employed as spacers or substrates in combination with metallic resonators. Furthermore, we explore the materials and types of geometry of dielectric resonators demonstrated for different applications in the terahertz regime. We contribute to the knowledge governing material selection, the fabrication techniques involved, and in certain areas propose novel techniques in the realization of these devices. The applications of dielectric materials either as dielectric substrates, spacers, or resonators have been widely discussed in other frequency regions, such as microwave and higher far-infrared (FIR) frequency.[24-30] Other reviews in the terahertz frequency have not particularly focused on the material properties and fabrication techniques of dielectric materials for terahertz devices. A detailed review of terahertz reflective and transmissive devices, their mode of operation and fabrication techniques given by Shi-Wei *et al.* did not specifically focus on dielectric materials and their different applications.[31]

Dielectric Materials as Spacers and Substrates at Terahertz Frequencies

Though Drude-type materials, such as noble metals and heavily-doped semiconductors exhibit high ohmic losses at terahertz frequencies,[23] a focus is still placed at realizing terahertz resonators with these materials in combination with dielectric spacers due to ease of fabrication with standard micro-fabrication techniques and acceptable efficiency.[21,22,32] The electromagnetic response of these devices when excited by an external electric field, is dependent on the conduction current on the metallic resonators and significantly on the degree of field confinement in the spacers carrying these resonators. Thus, the radiation efficiency is dependent on the losses in the materials constituting these devices.

Dielectric materials of desired relative permittivity values have been employed as spacers in single[33-40] and multilayer devices.[41-44] These devices have either been demonstrated as free-standing devices [33,37,43-46] or devices supported on a ground plane.[34-36,39-41,47,48] With a suitable dielectric material and shape of the resonating element, a wide range of applications can be demonstrated based on the manipulation of polarization,[36,37,41,44-46,49] phase,[36,40,48] and amplitude[33-35,38,39,43,47,50-52] of an incident electric field. Device demonstration examples include band-pass transmission;[33,43] broad- and narrow-band absorbers for detection applications;[34,35] low-loss polarizers;[36,45,46,53,54] low-loss and high-gain beamforming;[40,46,48,55] or devices demonstrating dynamic properties such as modulators and switches.[38,39,50,51]

Apart from radiation efficiency, the mechanical properties of the constituent dielectric spacers, as well as the fabrication techniques play an important role in realizing highly efficient terahertz devices.

In this section of the review article, we focus on fabrication techniques and choice of polymer materials for broader terahertz applications including free-standing (flexible and non-flexible) and substrate-backed, single- and multi-layer devices. Emphasis is placed on some very low-loss polymeric dielectric materials that have seen limited applications in the terahertz frequency. Novel fabrication techniques are introduced in the realization of high-efficiency devices. Most of these promising polymer dielectric materials and the fabrication processes were not discussed in a previous review on flexible terahertz devices.[32]

A wide range of materials can be suited for use as a spacer in a terahertz metasurface device, for a specific application. However, in order to realize practical efficient devices, a trade-off between the electromagnetic properties of these materials and other physical properties related to fabrication and subsequent integration must be taken into consideration. In selecting materials as dielectric substrates or spacers in terahertz devices, the following parameters should be considered:

- Optical properties such as low permittivity and loss tangent to support low dissipation across a broad bandwidth in the terahertz region.
- Thermal properties such as glass transition temperature and possibility of withstanding high temperature, preferably >400 ºC, required of integration steps and packaging.
- Low stress build up upon repeated heating during multilayer processing.
- Mechanical properties such as Young's modulus and stress to prevent cracks.
- Environmental stability such as resistance to acid, solvents, low water absorption, and retention of basic properties upon exposure to gases.
- Surface energy and roughness to support strong metal adhesion.
- Ease of fabrication.

Fabrication of single and multilayer terahertz metasurface devices

Flexible devices realized with polymeric materials

Polymeric materials have been widely employed for the fabrication of free standing and flexible terahertz devices mainly due to their low permittivity and low loss tangent.[32] These devices when bent to match conformal surfaces can reasonably retain their electromagnetic properties. Examples of most commonly used flexible polymer dielectric materials, as substrates or spacers, include polydimethylsiloxane (PDMS),[36,40,43,44,48] polyimide (commercially supplied as Kapton),[41,45,46,54] polyethylene terephthalate (PET), parylene-C,[34,56] cyclic olefin copolymer,[37,57] etc. The properties specific to each polymeric material and its challenges in fabrication are discussed and addressed.

General fabrication requirements

Most polymeric materials are commercially available under different trade names as a mixture of monomers and solvents in liquid form or as readily-made films. In liquid form, the layer is realized by spin–on techniques that involve spin coating the liquid mixture on a supporting ground plane prior to a heat treatment. Heat treatment removes solvent and crosslinks the monomer molecules to form films. As for readily-made films, the required dimension of the film can be cut and bonded to a ground plane or polymer-coated supporting wafer using heat treatment.

For free-standing devices, a sacrificial layer, e.g., polymethylmethacrylate (PMMA), a thin layer of photoresist, aluminium or platinum thin films, can be spun or deposited on a supporting wafer before bonding the desired film. The free-standing devices are realized after dissolving/etching the sacrificial layer. The sacrificial layer and film are thus chosen based on the resistance (selectivity) of the film (spacer) to the solvent used to dissolve the sacrificial layer. A review article by Walia *et al*. covers most commonly used polymer materials employed as support or spacers for terahertz flexible and

tuneable devices. Their electromagnetic and mechanical properties, tuneability, and methods of fabrication are discussed in the review.[32] Cunningham *et al*. presented spectroscopic data of refractive indices and absorption coefficients of a wide range of polymeric and organic films for broadband applications at terahertz frequencies.[58]

Polydimethylsiloxane (PDMS)

Polydimethylsiloxane (PDMS) has been employed as substrates in single layer terahertz devices[36,40,53] or as spacers in multiplayer terahertz devices.[43,44] The choice of PDMS is generally governed by low cost, ease of application by spin-on or drop cast techniques, and resistance to most solvents, acid, and basic mixtures. Its relative permittivity of 2.35 and loss tangent of 0.04 is comparable to most moderately low-loss polymer dielectric materials.[32] Moreover, PDMS is shown to have a moderate dissipation across the terahertz region, and can withstand processing temperatures between -50 ºC to 120 ºC. PDMS films are generally prepared by vigorously mixing a desired amount of silicone elastomer with a curing agent in various ratio depending on the desired stretchability. It is then left in a low pressure environment to remove air bubbles. The resulting liquid PDMS is spin-coated on a desired substrate. Curing of PDMS can be done in a preheated oven or hot plate at 100 ºC for 15 min or left naturally in an ambient condition for greater than 24 h. Free-standing PDMS-based devices can be released easily when spun on aluminium thin film-coated silicon wafer.[43] In one demonstration, PDMS nanocomposites with alumina nanoparticles or polytetrafluoroethylene (PTFE) inclusions are shown to exhibit a slightly lower dissipation than that of bare PDMS.[59] However, PDMS harbours some challenges due to its highly hydrophobic surface. This prompts extra fabrication steps such as UV flood exposure and oxygen plasma treatment to facilitate the adhesion of photoresist during photolithography patterning.

Polyimide (Kapton)

Polyimide is one of the most commonly used dielectric substrate or spacer for terahertz single[54] and multilayer devices.[41,45,46] The advantages include strong adhesion by metals and mechanical stability that facilitate terahertz device fabrication and resistance to solvents. It has a dielectric constant of 3.24 and loss tangent of 0.031 between 0.2 to 2.5 THz. However, these properties are shown to vary across 2.5 to 10 THz.[32,42] The operating temperature of polyimide dielectric films is between -269 ºC and 400 ºC.[32] Commercial polyimide films or sheets, known by its brand name Kapton, is commonly employed to realize terahertz devices. Its liquid counterpart, available as Dupont PI–2611 polyimide, allows for thickness control but the polymerisation process for cross-linking the monomers is performed at 400 ºC and associated to high water vapour release and generation of micro-voids in the films. For device fabrication, pre-made Kapton film of a desired size is cut and attached to a semi-

baked PMMA-coated support wafer prior to a standard microfabrication process. Upon completion of device fabrication, the polyimide film can be released easily by dissolving the PMMA in acetone to realise free-standing devices. Depending on applications, a metallic ground plane can be deposited directly on the back surface of the released film.

Parylene

Parylene is a flexible thermo-plastic that is usually applied for coating conformal sections of electronic devices. The many types of parylene revolves around the backbone structure of the phenyl ring 2.2 paracyclophane. Common examples include 2.2 paracyclophane dimer (parylene-N) or the inclusion of one or two chlorine (Cl_2) atoms in 2.2 paracyclophane for parylene-C and parylene-D, respectively. The dielectric properties of parylene-C has shown low-loss performance in the terahertz regime.[34,56] Moreover, it can withstand high temperatures in the range -200 ºC to 200 ºC. Parylene-C is stable in most solvents and can be released easily from surfaces by applying a water-soluble release agent prior to spin coating. A constant refractive index of 1.6 is measured between 0.45 and 2.80 THz for its variants parylene-C and parylene-D. However, both show an increasing absorption coefficient in the range of 2-11 cm^{-1}.[60]

Benzocyclobutene (BCB)

Benzocyclobutene (BCB) is a thermosetting resin that is widely employed for encapsulation of electronic components and in planarization experiments due to its mechanical and temperature stability. The relative permittivity and loss tangent of the commonly-used photosensitive BCB 4026-26[61] and non-photosensitive CYCLOTENE 3022-46,[62] are reported to lie in the range 2.41-2.65 and 0.002-0.009 at 1 THz, respectively. These low-loss dielectric material offer great opportunity to realize low insertion loss waveguides and other high-efficiency metasurface devices in the terahertz region.[63,64] The loss tangent of both BCB 4026-26 and CYCLOTENE 3022-46 cured films are experimentally shown to fluctuate with frequency in the range of 0.5-5.5 THz[61] and 10-50 THz,[62] respectively, with existing windows for low loss. However, the property of the film is dependent on the curing conditions such as the exposure fluence and duration, temperature, and degree of oxidation of the films. Low dispersion and low loss tangent are obtainable with a >95% monomer conversion associated to a heat treatment at 220-250 ºC for 30 min in a nitrogen-purged environment.[61,65,66]

Cyclic olefin copolymer (COC)

Cyclic olefin copolymer (COC), often also called cyclo olefin copolymer, is a relatively new class of polymeric compound in contrast to traditional propylene and ethylene compounds. COC is gaining

attention due to its very low loss across the entire terahertz frequency region.[42] COC is commercially produced under the trade name of TOPAS from polymerisation of a mixture of monomers (co-polymerisation) including ethylene. Generally, cyclic olefin polymers (COP), involving just one monomer and COC are often employed as a thermal nanoimprint resist for micro-fabrication, by injection moulding techniques.[67] COC has an absorption coefficient and loss tangent of $\alpha = 0.2$ cm^{-1} and $\tan\delta = 7 \times 10^{-4}$, respectively, at 1 THz, which is three orders of magnitude lower as compared to those of frequently used polymeric substrates. COC also has a constant refractive index over a broad bandwidth, can be spun to different thicknesses and can be treated with low to high processing temperature based on the glass transition temperature.[58,68] Due to its extremely low loss tangent, biocompatibility, and high chemical stability, COC has been employed as substrate material in polarizers,[37] antennas,[57] microstrip lines and grounded coplanar waveguides,[69] aperture and free-space mesh filters,[33,42] bendable polymer-type terahertz photonic crystal fibres,[70] and widely as microfluidic channels for lab-on-a-chip devices.[71]

However, application of COC is curbed with adhesion challenges with respect to metal resonators and to ground planes. Solutions such as oxygen plasma or UV treatment of COC and direct deposition of gold (Au) resonators on COC, have been proposed.[68,72,73] Exposing or immersing COC to a mixture of a polar solvent, such as, acetone, or, a nonpolar solvent, such as, cyclohexane, have also been proposed for biochemical applications where heat or plasma treatment is not favored.[74] However, these techniques are not suitable for multilayer devices that involve multiple patterning steps. Secondly, chemical treatment of COC can introduce stress or gas bubbles that will greatly attenuate terahertz signals *via* wave scattering.

Patterning resonators of gold thin films on spin-on COC can be successfully achieved (**Figure 1**a,b) and extended to multi-layer structures (Figure 1c). Pavanello *et al*. reported a double-layered terahertz mesh filter in which the second patterned resonators were laid on a COC spacer that was prepared by direct spin-coating of liquid COC on the first layer resonators and cured by heat treatment (Figure 1d).[42] Our experimental work has found that liquid COC instantly dissolves the cured COC upon contact, thereby displacing the initial patterned resonators during spinning. This is probably due to the presence of nonpolar constituent solvents in liquid COC that easily penetrates cured COC. Figure 2 presents the fabrication process of multilayer devices based on COC. A fabrication sequence is described in the figure caption.

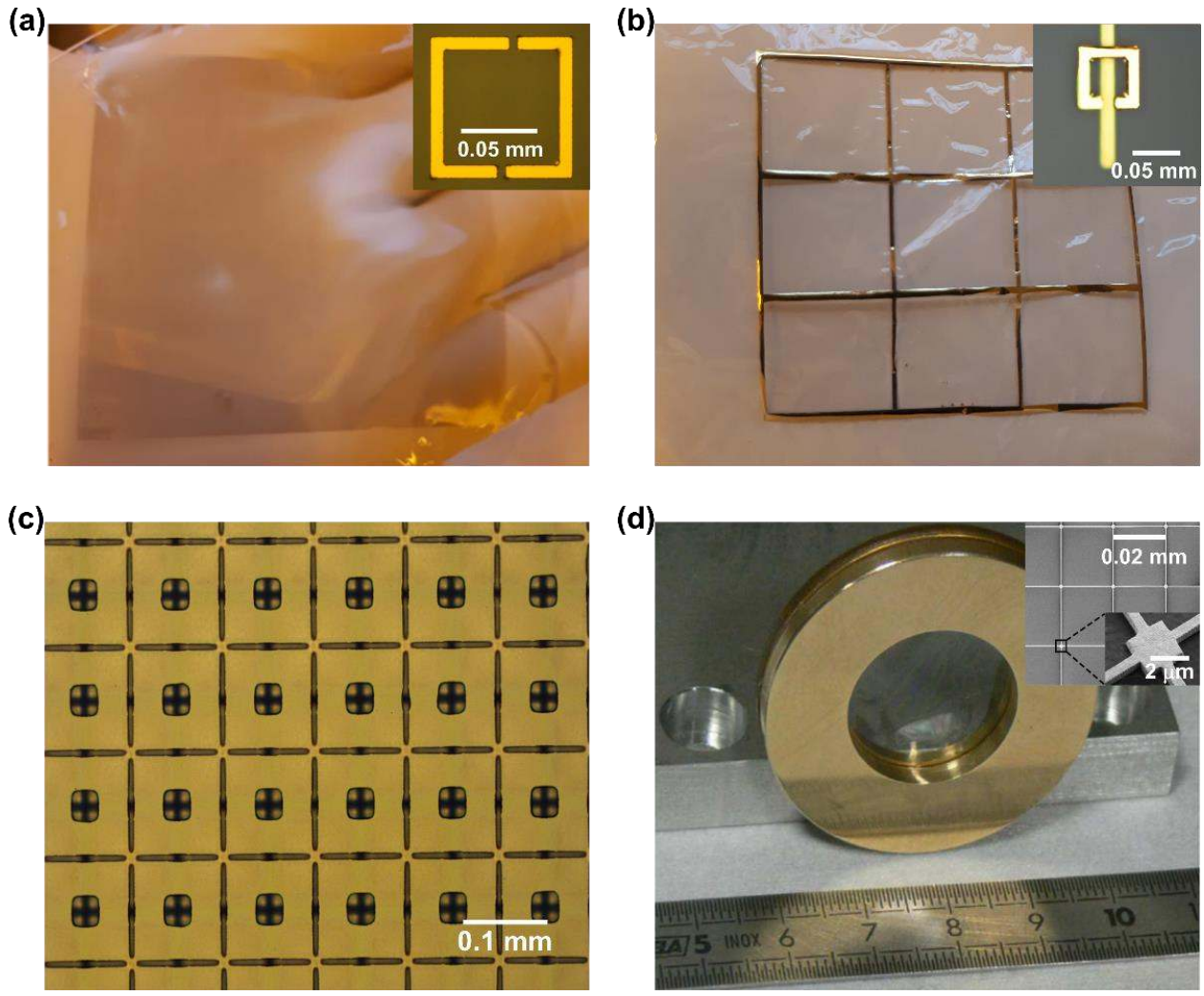

Figure 1 | Single and multi-layer devices based on COC. (a) Optical image of single-layer free-standing split ring resonators (SRR) (shown as inset) on COC. (b) Double-layered 5.2 μm thick metamaterial. The grids represent different distortion of the strip resonator from the SRR ring gap, as shown in the inset, with COC as dielectric spacer. (c) Double-layer narrow-band absorber on a gold ground plane with COC as spacer. (d) Photograph of a single-layer frequency-selective grid metasurface (inset) employing COC. Reproduced with permission [42] copyright 2013, Applied Physics Letters.

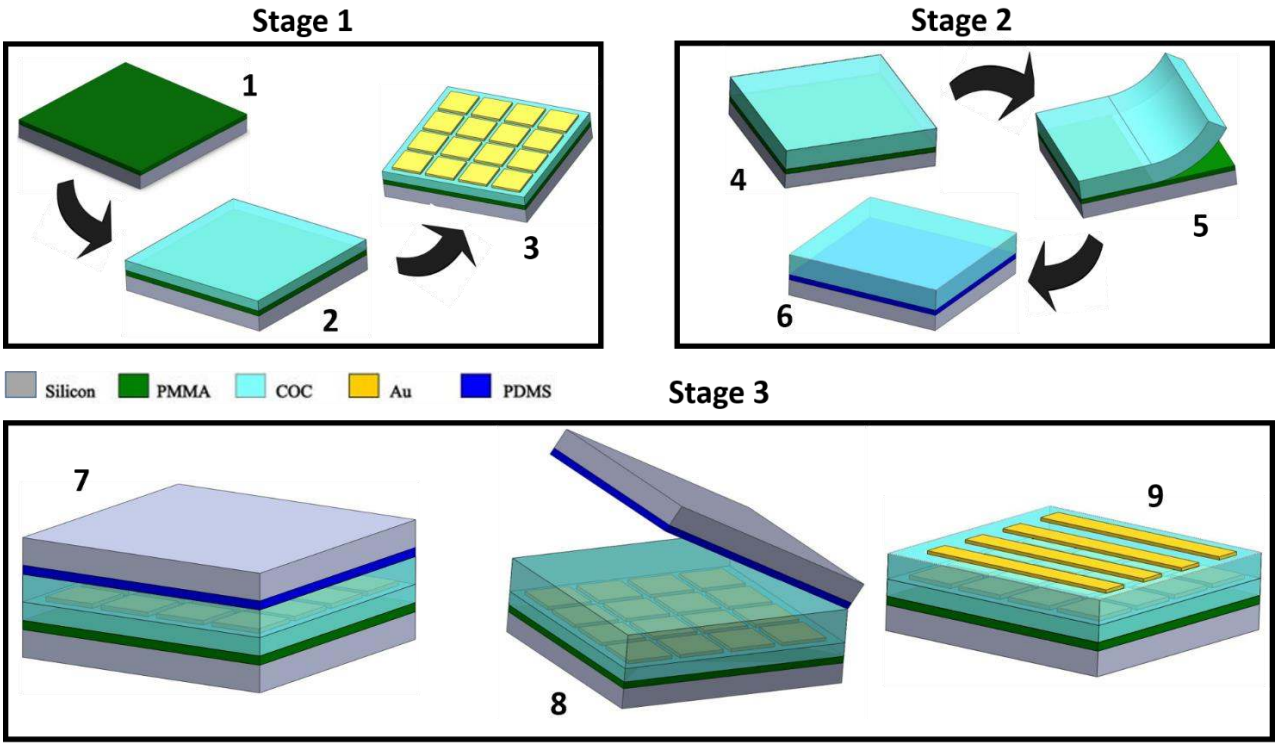

Figure 2 | Fabrication of multi-layer devices based on COC. (Stage 1) PMMA is spin-coated on a supporting substrate (3" Si wafer) and dehydrated at 120 °C (1). COC is then spin coated on the PMMA/Si wafer (2). Followed by patterning and deposition of 1st layer Au resonators (3). (Stage 2) Stage 2 is carried out on a different wafer. First, COC is spin-coated on a PMMA-coated 3" Si wafer (4). Free standing COC is released (5), and attached to a PDMS-coated 3" Si wafer (6). PDMS facilitates release and is unaffected by subsequent heat treatment. (Stage 3) Next, COC/PDMS/Si wafer is placed on the 1st layer Au resonators (7). Bonding is performed at 100 °C, 400 N and a dwelling time of 15 min using a wafer bonder (SB6 SUSS Microtech). Bonded COC is released easily by peeling off the PDMS-coated wafer (8). 2nd layer Au resonators can then be patterned and deposited easily (9). Stages 2 & 3 can be repeated to fabricate 3 or more layered metallic resonator COC based devices.

Table 1 presents the electromagnetic, chemical and physical properties of most often used low loss dielectrics for terahertz application.

Table 1 | Comparison of physical, chemical and electromagnetic properties of commonly used low loss dielectric materials for terahertz applications. ε_r - relative permittivity; tan δ – loss tangent; T_g – glass transition temperature; T_t – curing temperature.

Dielectric material	**Electromagnetic property**		**Chemical properties**	**Physical properties**		**Ref.**
	ε_r	tan δ	Water absorption (%)	T_g (°C)	T_t (°C)	
Polydimethylsiloxane (PDMS)	2.35	0.04	Very hydrophobic	123-127	150	[59,75-77]
Polyimide (Kapton)	3.24	0.31	N.A	N.A.	400	[58]

Parylene	2.43	0.04	0.01(N); 0.06(C); 0.1(D)	200-250 (N) 150 (C)	200	[60,78-80]
Benzocyclobutene (BCB)(Cyclotene® 4026-46; BCB 4026-26; CYCLOTENE 3022-46)	2.41-2.46	0.002-0.009	0.25-1.4	250	220-250	[61,65,81,82]
Cyclic olefin co-polymer (COC)	2.3	0.0007	<0.01	85-132	140	[67,71,73,81]

Non-flexible polymeric and non-polymeric spacers

Other dielectric materials applied as spacers in the fabrication of terahertz metasurface devices due to their low loss, availability or ease of handling include sapphire,[39] F4B-2,[83] FR4,[55] SiO_2, and silicon nitride (Si_3N_4).[35] Dynamic modulation and tunability has been demonstrated with doped semiconductors[38,39] and two-dimensional materials (graphene) assisted spacers.[50,51] Most of these materials can be applied by conventional thin film deposition techniques such as electron beam deposition, sputtering, or plasma-enhanced chemical vapour deposition (PECVD). For high purity, specific doping concentration and uniformity requirement, thin film growth techniques such as metal-organic chemical vapour deposition (MOCVD) for doped-Si and graphene can be utilized. While these materials have high relative permittivity, they do involve very expensive and demanding processes.

Dielectric Materials as Resonant Elements and Structures

Moderate to high relative permittivity dielectric materials can be designed to support resonance modes at a specific frequency through field confinement in the form of displacement current. Depending on the intrinsic loss of material, this would result in high energy dissipation in the material or radiated to free space.

Typically, the real part of the permittivity is the degree to which a materials molecular structure can be polarized with regards to atomic scale displacement, when an external field is applied. An incident electric field causes a displacement current attributed to the collective oscillatory motion of polarized atoms/ions. The incident energy is both stored (“captured”) and radiated when an external field is applied. The Q factor is a ratio of energy stored to the power dissipated *via* material losses and

radiation. This is dependent on the complex permittivity and other near-field parameters such as periodicity.[84] Dielectric materials with high relative permittivity weakly couples with an excitation, with tendency to be engineered for high-Q devices.[85] Those with low relative permittivity strongly couple when excited with an external electromagnetic wave. Low-Q dielectric resonators can support broad bandwidth operation with less sharp resonance and smooth phase change.

Subwavelength structures composed of dielectric materials have been engineered for device-specific applications at the terahertz regime. On one hand, low-loss dielectric materials with moderate to high relative permittivity have been engineered into metasurfaces as phasing elements with nonuniform dimensions for wavefront manipulation and dynamic beam control for antennas and lenses.[86-94] or with anisotropic properties for polarization manipulation.[95-98] On the other hand, lossy dielectric materials with moderately high relative permittivity are engineered to enhance coupling between and field confinement within subwavelength resonant cavity bodies. Such materials can also be designed to confined fields and subsequently dissipate in resonators for broad band terahertz absorbers.[99-107]

As guidelines to the choice of these group of dielectric materials, we look at a wide range of properties including:

- Moderate complex permittivity that defines quality factor of dissipation Q_{dis} and quality factor of radiation Q_{rad}, based on device specific application
- Mechanical properties – Young's modulus and stress-based cracks generation
- Retention properties upon wetting and exposure to gases
- Fabrication – based on ease to design geometry and further integration
- High selectivity and availability of gas chemistry and mask for semiconductor processing
- High thermal stability and possibility of integration

Lossless dielectric materials

Dielectric materials with low loss tangent and moderate to high relative permittivity support high radiation efficiency across the terahertz frequency region. Resonators made of such materials can be designed to exhibit high absorption quality factors (Q_{abs}) and moderately low radiation quality factor (Q_{rad}) for wide band applications.[108]

High-resistivity, single crystal float-zone silicon (HR Si) is the most widely employed low loss dielectric material as resonators for free-space devices. This is due to its low loss, moderate to high dielectric constant, stable properties across a range of wavelengths, ease of etching unit structures using deep reactive ion etching (DRIE) processes,[86-91,93] and ease of handling. Intrinsic Si has a purity level dependent loss tangent $\tan\delta < 4 \times 10^{-5}$ and moderate relative permittivity (ε_r) of 11.68 at 1 THz. The absorption coefficient is less than 0.05 cm^{-1} in the terahertz range. The disadvantage of

using high-resistivity Si resonators has been the difficulty to realize devices on different substrate material for both reflective and transmissive devices.

Though the application of high-resistivity Si as resonators is just gathering steam in the terahertz region, their application for beam focusing, beam shaping, and polarization control has been reported in the microwave[109,110] and optical frequency ranges.[111-113] Of particular importance to this review is the fabrication steps that rely mostly on deep reactive ion etching processes used to define the structured devices, given in a later section. Moreover, novel practices to overcome limitations in realizing reflective devices in the terahertz frequency region is proposed based on eutectic bonding. This is also discussed in detail in a later stage under fabrication methods. Hereafter, we highlight some of the work demonstrated in the literature employing dielectric material-based resonators for beam focusing, shaping, and polarization control.

Reflectarrays for focusing and beam shaping

Beam shaping, also termed wavefront engineering, is the informed manipulation of field distributions to achieve a desired near-field or far-field pattern. Such patterns include beam collimation, Bessel beam, beam steering, focusing beam. Beamforming can be attained by designing a spatial phase response across a metasurface.[48,114] In the context of this work, when excited by an electric field, dielectric resonators of a specific dimension, on resonance can support in-phase oscillations with 0º reflection phase that couple coherently with free space. As the dimension of the resonator gradually changes, the reflection phase gradually deviates from 0º. The reflection phase can thus be tuned by changing the resonator dimension. A nearly full 360º phase control can be achieved discretely by engineering the metasurface device with an array of selected dimension of dielectric resonators, for beam shaping and beam focusing. The advantage of using dielectric resonators is the smooth phase control, as compared to metallic resonators. The use of dielectric resonators to design non-uniform metasurfaces with gradual phasing elements for beam focusing and beam shaping at terahertz frequency has been widely demonstrated.[86,88-94] Headland *et al*. designed non-uniform high-resistive Si cylinders with varying diameter on a ground plane. These were fabricated by employing SU-8 to bond the high resistive Si to a Au-coated standard Si substrate, before deep reactive etching (**Figure 3**a).[86] Ma *et al*. also fabricated a reflective mode phase control metasurface realized with high resistive Si cubes on SiO_2 insulator (deposited by inductive coupled plasma chemical vapour deposition) bonded to fused silica substrate, with the help of UV curable polymer (Figure 3b).[87] On the other hand, transmission mode phase control dielectric resonators-based devices have also gained attention due to their ease of use.[88-93] Jiang *et al*. demonstrated beam focusing metalens in transmission mode using oriented Si rectangular cubes etched on SiO_2 that is bonded to standard Si as substrate (Figure 3c).[88] Huifang *et al*. demonstrated high-efficiency polarization-dependent wave

control in transmission mode using cylindrical Si resonators on Si substrate (Figure 3d).[89] In another article, they demonstrated polarization-dependent terahertz wavefront control in transmission mode using rectangular high-resistivity Si resonators with variable side lengths etched on a Si substrate (Figure 3e). High-resistivity Si pillars are also engineered on the opposite side to curb reflection losses.[90] Jia *et al*. also demonstrated a transmission mode full phase control with a metasurface composed of a spatial distribution of cross-shaped high-resistivity Si resonators etched on Si substrate. The length of one of the cross-arms is varied across the metasurface to control phase profile (Figure 3f).[91,92] Lee *et al*. also designed and demonstrated in transmission mode high-resistivity Si on quartz substrate by SU-8 assisted bonding, to study near field electric and magnetic resonances.[93]

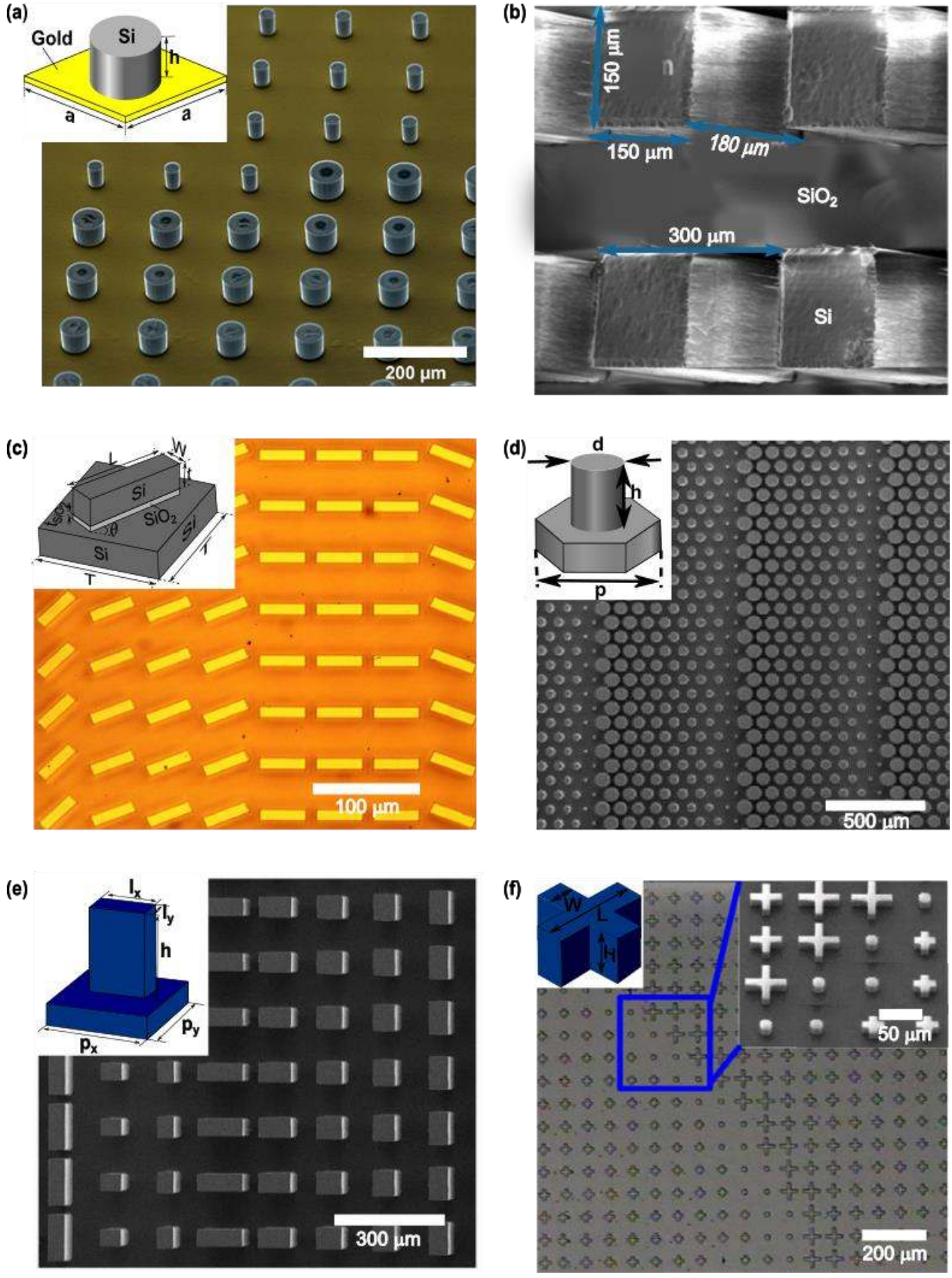

Figure 3 | Dielectric resonators for wavefront manipulation. Scanning electron and optical micrographs of various dielectric resonators devices, all utilizing intrinsic silicon, with appropriate unit cells shown as insets. (a) Cylindrical resonators for beam focusing at 1 THz. A distribution of cylinder radii (h = 50 μm) show 18% bandwidth at 150 mm. (b) Cubes (pillars) etched on deposited SiO_2 with cube dimensions of

150×150×180 μm^3 used to experimentally demonstrate close to unity reflection coefficient. (c) Rectangular cubes inclined at different angles to a plane perpendicular to the surface of the metalens. (d) Pillars on a hexagonal lattice for anomalous deflection. (e) Section of a fabricated polarization beam splitter composed of a distribution of rectangular-shaped pillars of varying width and length. (f) Spatial distribution of cross-shaped resonators with varying arm length to achieve a smooth 2π phase profile. Figures adapted and reproduced with permission (a)[86], copyright 2016, American Chemical Society, (b)[87], copyright 2016, American Chemical Society (c)[88], (d)[89], copyright 2018, Chinese laser press (e),[90] copyright 2017, Advanced Optical Materials, John Wiley and Sons, and (f)[91,92] copyright 2017 OSA.

Polarization manipulators

Polarization manipulation adds a great degree of freedom in utilizing terahertz waves in various applications. As opposed to conventional polarizers or waveplates, the concept of metasurfaces allows designable birefringence with great flexibility. Particularly, dielectric resonators can also be engineered to exhibit birefringent response. Wherein, when excited with electromagnetic waves, the resonators couple strongly with the electric field and a significant phase change is induced on either of the orthogonal polarization counterparts of the incident electric field. The metasurface can thus be engineered as a half waveplate (HWP) or quarter waveplate (QWP) with 90º or 180º phase difference, respectively. In this way, the fundamental frequency of resonance and the device efficiency, are dependent on the resonator structure and dielectric material used. As a result, dielectric resonators made of different materials have been designed in different shapes to interact differently to the two orthogonal polarizations of an incident wave for linear to linear polarization rotation,[95-98] linear to circular,[95,96] and circular to circular polarization conversion with preserved handedness.[95] Irrespective of the mode of operation (reflective or transmissive) the materials used are designed to exhibit low dissipation and high radiation losses for efficient output or conversion, as discussed earlier.

Lee *et al*. designed and experimentally validated the polarization response of 'sine' curved blocks (**Figure 4**a) and meander line (Figure 4b) from intrinsic high-resistivity Si (>5 kΩ·cm) resonant structures in reflection mode by means of eutectic bonding, for linear to circular and linear to linear polarization conversion, respectively.[95] Chen *et al*. have employed inductive couple plasma etching of high-resistivity Si (>10 kΩ·cm) to realize a periodic (Figure 4c) and monolithic (Figure 4d) gradient grating to rotate linearly polarized terahertz wave by 90º in the frequency range 0.6 to 1.4 THz.[96] Zi *et al*. designed and experimentally validated a two-layer transmissive linear to linear polarization rotator with a low-doped (p-type) Si of resistivity 1-3 kΩ·cm and thickness of 2 mm (Figure 4e). Deep reactive ion etching and wet etching of Cr mask were used to realise elliptical and rectangle pillars on both sides of the p-type Si wafer to act as linear to linear polarization rotator and antireflection layers, respectively.[97]

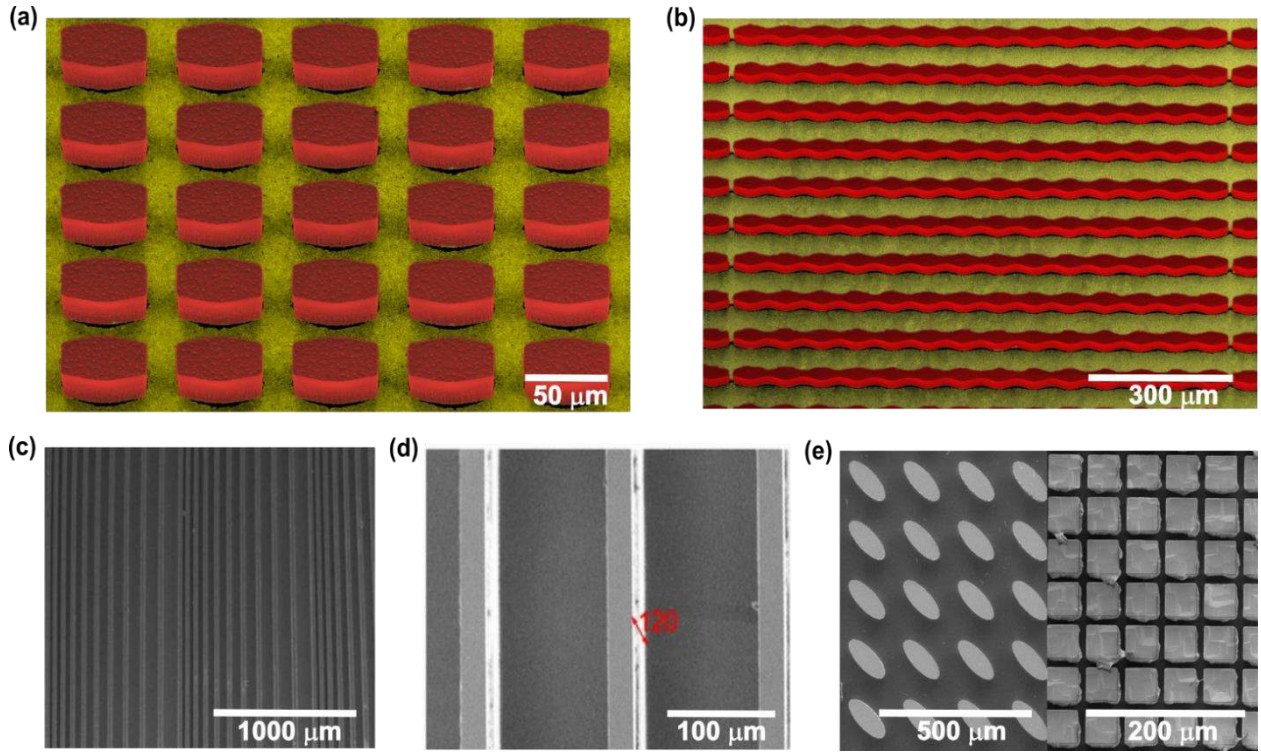

Figure 4 | Dielectric resonators devices for polarization control. Scanning electron micrographs of polarization conversion devices based on dielectric resonators, all using silicon. (a) Quarter waveplates and (b) half waveplate defined by etched high resistivity Si structures bonded to a Au ground plane by eutectic bonding. (c) Periodic gradient grating and (d) monotonic gradient grating etched in high resistivity Si. (e) Transmissive half wave plate composed of elliptical doped-Si pillars as the half wave plate layer (left pane) and Si square pillars as antireflection layer (right pane). Figures adapted and reproduced with permission, (a) and (b),[95] copyright 2018, OSA, (c) and (d),[96] (open rights) and (e)[97] copyright 2018, AIP Publishing.

Lossy dielectric materials

Dielectric materials with high loss tangent and moderate to high relative permittivity can be used to create resonant cavities. These resonators support strong energy trapping enhanced by a non-radiative damping behaviour. The size, shape and material choice of such resonators is focused towards realizing localised surface plasmon resonance (LSPR).

Moderately-doped Si, III–V compounds such as indium antimonite (InSb),[104] and oxides such as titanium dioxide (TiO_2) and vanadium dioxide (VO_2) are predominantly lossy at terahertz frequencies attributed to the scattering behaviour of free charge carriers. The plasma frequency of such dielectric materials can be adjusted by doping for operation at terahertz frequencies. The transmission and reflection coefficients of metasurfaces employing such lossy dielectric material are thus dependent on the amount of doping concentration and/or external stimuli, such as heat, optical pump, or voltage bias. On one hand, resonators of different shapes and sizes of such semiconductor materials have been designed to support high field confinement for perfect absorption of terahertz radiation. While on the

other hand, the electronic properties or electronic band structure of such dielectric materials with moderately high dielectric constant and low loss tangent can be tuned by an external stimulus, such as light, temperature, and electrical bias. The modification of recombination sites by impurity atoms or surface chemical treatment to realize active devices is also attainable.

Terahertz absorbers

The absorption mechanism of earlier designs using metallic resonators have been explained in several ways. It can be described as the manipulation of electric and magnetic resonance of a metasurface to match free-space impedance with high dissipation on resonance; or as the engineering of metasurfaces to exhibit multiple reflection with a resulting destructive interference in the direction of reflection/transmission; or as the generation of an out-of-phase reflection at the metasurface–air boundary from the combine effect of electric and magnetic surface currents on the metasurface resonators, on resonance. Doped dielectric resonators, *e.g*., doped Si, exhibit metallic behaviour and support LSPRs in confined cavities or delocalized in-plane SPP, on resonance. Examples of engineered dielectric material-based resonator geometries include micro-cylindrical cavities,[99,100] cylinders,[102] cross-shaped,[103] disks,[104] sawtooth,[105] microspheres, etc. have been demonstrated for perfect absorption of terahertz radiation. Heavily-doped Si has seen wide application in this respect due to ease of fabrication based on its crystallographic nature. The standard fabrication methods to realise these structures are either wet chemical etching or deep reactive ion etching (DRIE) processes that are discussed in detail below.

Lossy plasmonic resonance was demonstrated by using an array of blind annular holes etched into doped silicon (annular microcavities) for perfect terahertz absorption (**Figure 5**a). The field confinement and strong field strength within the annular cavities support guided modes with resonance dependent on the depth and separation of the sidewalls.[99,100] Square-shaped doped-silicon structures caped with SU-8 dielectric layer having four-fold symmetry is shown to enhance dissipation with incident angle insensitivity (Figure 5b).[101] Fan *et al*. have also demonstrated a high-efficiency terahertz absorber composed of 212 μm wide cylindrical resonators on 8 μm PDMS substrate with peak absorption efficiency of 96% around 0.6 THz (Figure 5c).[102] Cheng *et al*. designed and experimentally validated a plasmonic absorber using a 2D array of cross structures that support distinctive plasmonic modes as a result of high field confinement between adjacent arms and within cavities formed by the four adjacent arms, that greatly enhance the absorption bandwidth (Figure 5d).[103] Touching geometrical indium antimonite (InSb) disks on a semi-insulating gallium arsenide (GaAs) substrate are demonstrated to exhibit strong field confinement in areas where the two cylinders overlap. The degree of overlap of the two disk dimers is shown to have a strong effect on the absorption cross-section and is polarization sensitive (Figure 5e).[104] Titanium dioxide (TiO_2)

patterned microspheres on an aluminium film (Figure 5f) are also demonstrated to exhibit Mei resonances related to the size, mean permittivity, filling factor, and dispersity of the microspheres.[115]

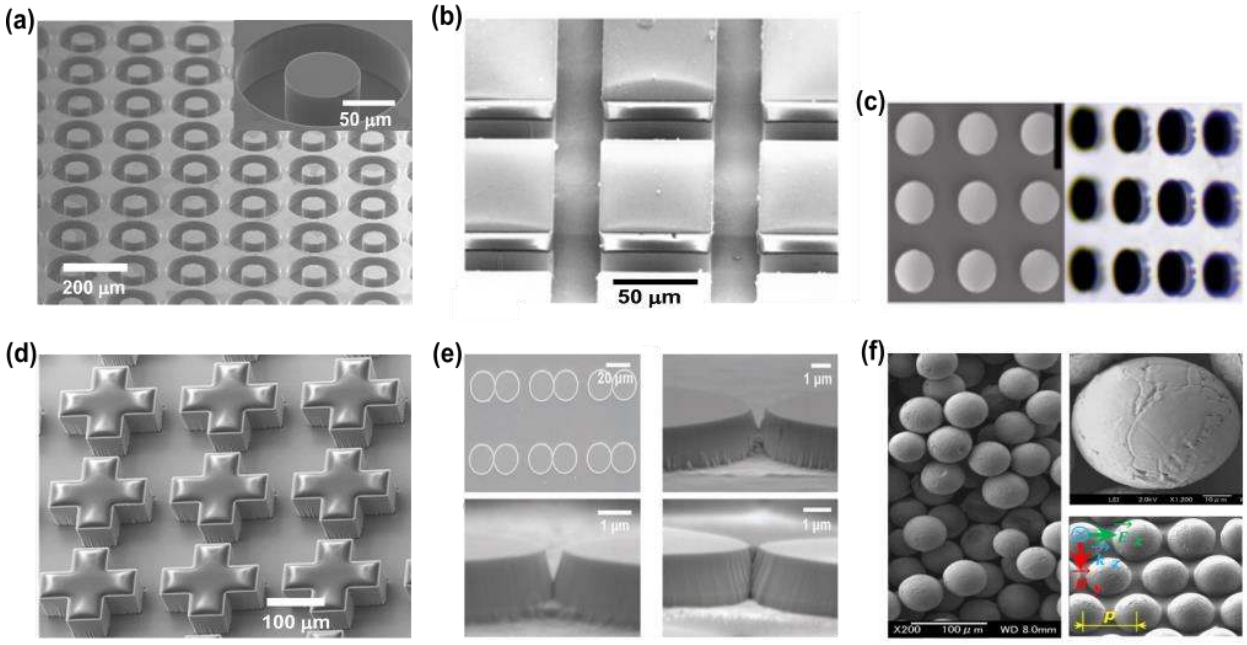

Figure 5 | Dielectric resonators for terahertz absorbers. A collection of scanning electron micrographs for different absorber structures utilising a variety of dielectric materials are presented. (a) Coaxial microcavities realised by Bosch DRIE into phosphorus (n-type) doped Si. (b) Square phosphorous-doped silicon patches with SU-8 capping layer. (c) Free-standing n-type Si cylinders realised DRIE on standard Si and transfer process on PDMS. (d) Cross-shaped resonators realised by Bosch DRIE into phosphorus (n-type) doped Si. (e) Overlapping InSb disks with three different overlaps, with top-left panel showing top view of an array of the disk dimers. (f) TiO_2 microspheres (left panel, as purchased) are uniform (top right) and defined as a 2D array of microspheres (bottom right) by sprinkling TiO_2 microspheres on Al adhesive tape. Figures adapted and reproduced with permission: (a),[99,100] copyright 2013, Advanced Optical Materials, John Wiley and Sons (b),[101] copyright 2015, AIP Publishing, (c),[102] copyright 2017, OSA, (d),[103] copyright 2014, Advanced Optical Materials, John Wiley and Sons (e),[104] copyright 2012, Advanced Optical Materials, John Wiley and Sons and (f)[115] copyright 2015, OSA.

Active tuning of dielectric-material-based resonators

Semiconductors defined by a charge carrier density, radiative and non-radiative recombination states, direct bandgap, temperature-induced phase transition, or a space charge region fall in this category. Such materials can be engineered in an array configuration to modulate the transmission and reflection amplitude, phase or polarization of an incident terahertz wave, or actively switch resonant frequency. In this category, moderately-doped silicon,[106,116,117] compound III–V semiconductors,[56,118] two-dimensional materials and van der Waal heterostructures,[119] III–V

semiconductor and carbon nanotubes and nanowires,[56,118,120-122] and oxide nano-spheres[123] have been demonstrated to exhibit active response in the terahertz regime.

For such an array of resonators, the resonance frequency is dependent on the LSPRs that are excited by an incident wave. This in itself is dependent on the geometry and electronic properties such as charge carrier density, mobility, and effective mass of electrons of the semiconductor.

Intrinsic silicon is lossless and to exhibit ohmic behaviour (to possess enough surface charge conduction that can couple strongly to free space excitation) its charge carrier density and mobility must be altered desirably. In one approach, a pump can be used to excite a semiconductor with different power to excite hot carriers by thermalization and diffusion which can then be probed with a terahertz beam. When probed, the excited charge carries can collectively oscillate and couple with free space radiation as LSPRs, and thereby, radiate or increase field confinement of terahertz radiation. Thus, the degree of coupling with free-space radiation can be regulated allowing for active control of an incident wave.

Berrier *et al*. showed the permittivity as a function of frequency for different carrier concentration in Si. In their study, active control of extinction ratio as a function of frequency of an incident wave is demonstrated with an aperiodic array of Si bow tie resonators, fabricated from undoped and n-doped silicon on fused silica using wet etch and DRIE techniques (**Figure 6**a(i)). Increasing the pump fluence increases the carrier density thereby increasing field confinement in the base and gaps between the resonator pair forming the bow tie (Figure 6a(ii)). This increases the lifetime and strength of the extinction peak. [124] Moreover, the enhanced field confinement resulting from doped Si bowtie antennas has been employed as a thickness dependent sensor for TiO_2 and SiO_2 thin films (Figure 6a(iii)), as the resonant frequency is blue-shifted with increasing thickness (Figure 6a(iv)).[116] Deng *et al*. designed and demonstrated experimentally that Indium Antimonite (InSb) grating grooves etched on semi-insulating gallium arsenide substrate (Figure 6b(i,iii)), can modulate the transmission coefficient of an incident terahertz wave when optically pumped with 405 nm femtosecond laser, (Figure 6b(ii)). By gradually increasing the laser fluence, an increasing charge carrier density on InSb increasingly attenuates incident terahertz radiation and reduces transmission (Figure 6b(iv)). A modulation speed of 1.2 GHz, approximated to 46%, is attributed to the picosecond time scale decay for the excited charge carries due to surface recombination sites.[125] Baig *et al*. have demonstrated terahertz transmission and polarizer modulation realized with aligned GaAs nanowires embedded in parylene-C (Figure 6c(i,ii)). The anisotropic geometry, high charge carrier mobility and ultrafast carrier charge decay of GaAs nanowires embedded in parylene-C, is utilized to modulate the polarization (Figure 6c(iii)) and transmission intensity (Figure 6c(iv)) of an incident terahertz beam, enabled by a polarization dependent light pump and fluence between 6 and 28 $\mu J/cm^2$.[56]

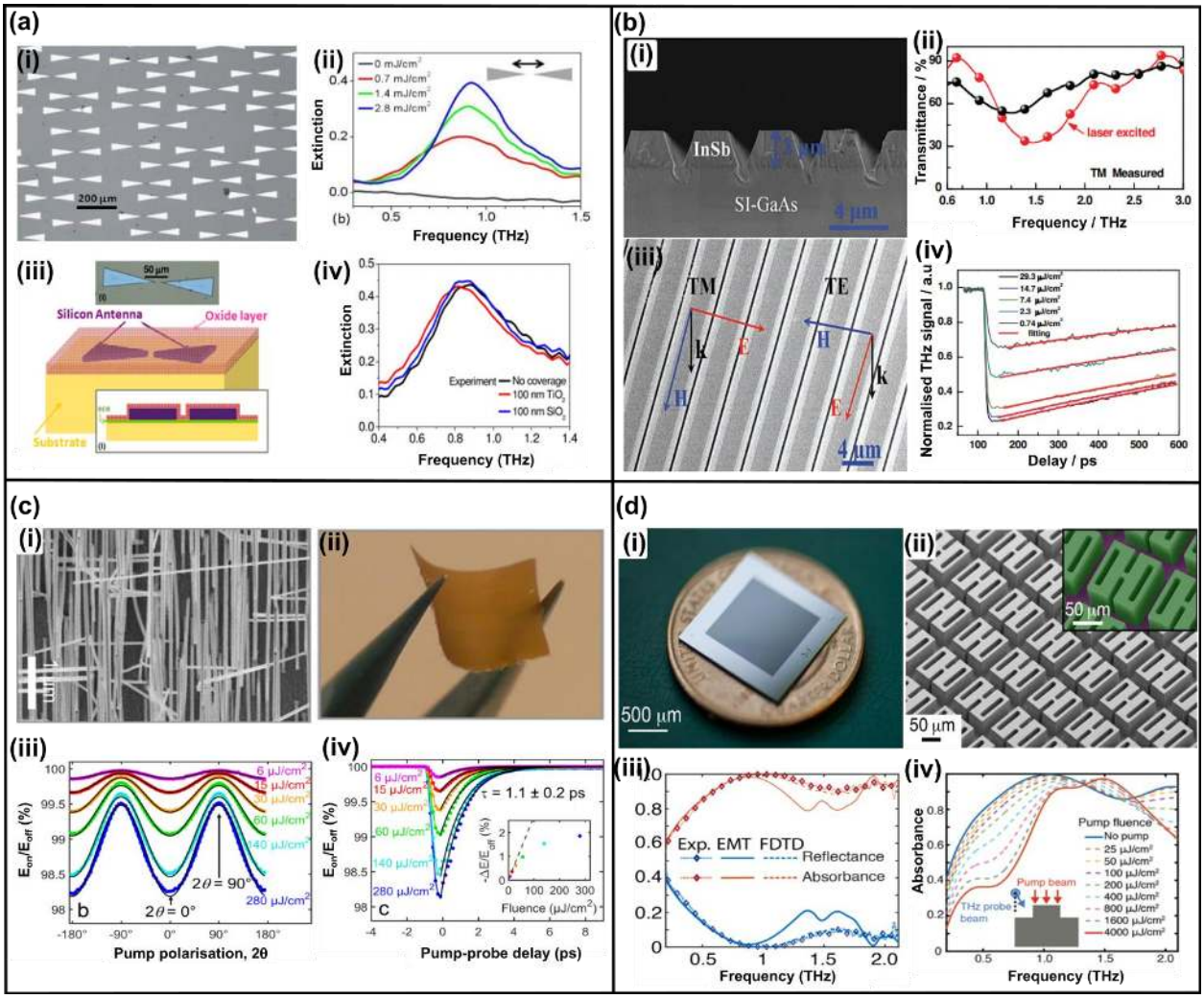

Figure 6 | Dielectric resonators for active terahertz wave control and tuneability. (a) Bow tie antennas of Si on SiO_2 on quartz: i. optical micrograph, ii. Normalised amplitude extinction spectra, iii. Device schematic, and iv. influence of addition of oxide dielectrics. (b) InSb gratings on GaAs: i. side-view, ii. measured transmission without and with laser excitation, iii. isometric view, and iv. normalised transmission against delay time for different fluence. (c) Vertically aligned GaAs nanowires: i. electron micrograph, ii. fabricated device on parylene-C, and terahertz transmission as a function of iii. pump polarisation and iv. pump–probe delay. (d) Metamaterial perfect absorbers based on doped-Si: i. optical image, ii. scanning electron micrograph, iii. measured and simulated absorbance, and iv. optical pump and terahertz probe absorption spectra metamaterial perfect absorber sample for different pump fluences, (a),[116,124] copyright 2012, OSA, (b),[125] copyright 2013, Advanced Optical Materials, John Wiley and Sons (c),[56] copyright 2017, American Chemical Society, and (d)[107] Copyright 2019, American Chemical Society.

Fabrication of dielectric resonators based devices

Dielectric-based devices are often fabricated by micro fabrication techniques involving etchant gases or liquids, used to transfer pre-patterned structures to the dielectric bulk material. The standard fabrication procedure involves, a pre-patterning step that defines structures on the dielectric surface using photolithography and/or deposition techniques (for hard masks), repeated exposure to etchants

(ionized gases or liquid reactants), a cleaning step to remove residuals and subsequent dicing to define specific device structure. Two main groups of etching techniques exist: liquid-based (wet) and gaseous-based (dry) etching.

Dielectric devices fabricated using the liquid-based technique often involves more stringent measures. In a typical procedure, the pre-patterned dielectric material is repeatedly immersed in a solution of liquid reactant that selectively dissolves the exposed dielectric material. High selectivity between the mask, the dielectric material and the supporting substrate (if any) is highly desired for well-defined feature profile. Meanwhile, the feature profile is also dependent on a number of other factors, such as, rate of immersion in the etchant, temperature, mask hardness and pre-treatment of the dielectric material surface.

However, wet etching is prone to high defect levels on the feature side walls and is inadequate for sub-micron features. Moreover, the process entails close proximity with highly corrosive etchants and easily involve toxic by-products. Due to these issues, the technique is mostly used for noncritical processes such as Radio Corporation of America (RCA) cleaning (removal of SiO_2 layer to obtain clean Si wafers) and masks for DRIE processes. Herein potassium hydroxide (KOH) and hydrofluoric acid (HF) are used to etch Si and SiO_2 materials, respectively.[124] For example, etching of crystalline silicon is usually anisotropic as etchants like KOH display a crystallographic orientation-dependent etch rate selectivity. This creates crystal plane boundaries resulting to a trapezoidal or pyramidal cross-section.

On the other hand, dry etching is a predominantly plasma etching process that physically erodes the exposed dielectric using energized ions from gaseous state. Such a technique is more controllable due to precise control of process parameters such as temperature, pressure and cross contamination (introduction of impurities), as well as, excellent profile results and reproducibility. For example, deep reactive-ion etching (DRIE) that involves the use of highly directed energized ions (from ignited gases) in low pressure chamber, is highly unidirectional, resulting to nanometer scale features with high aspect ratio. In particular, the Bosch process is a common technique adapted to etch Silicon. A combination of sulphur hexafluoride (SF_6) and octafluorocyclobutane (C_4F_8) is employed to erode, and at the same time, passivates (protect the walls), respectively. The combine process enables a more vertical than lateral excavation, thereby promoting an anisotropic etching. SF_6 operates in two stages; a short burst ensures the removal of the passivation layer, mostly in the vertical direction, while a more stable ion beam excavates the underlying silicon. An ideal or properly regulated etching process does not or only partially erodes the passivation layer deposited on the walls, resulting to perfect vertical etched-profile. A wide range of dielectric–based resonators composed of Si resonators have been realised for different applications using the Bosch DRIE process that employs fluorine-based

chemistry.[86,90,95-97,99,100,103,117] Chlorine-based chemistry, such as Cl_2 and BCl_3, is employed to etch III–V compound materials based on the non-reactivity of fluorine to indium-based compounds and the high mass transfer rate required for the removal of indium-based by-products.[104]

Micromachining or laser patterning

This is also similar to etching where a specific pattern, designed schematically (using instrument-specific software), is engraved onto a material using automated machine tools or laser pulses. In laser patterning, ultrafast lasers evaporates the designated areas on the surface of the dielectric, capable of creating features down to sub-micron scale and good side-wall profile. Adequate cooling and suction conditions are put in place to prevent heat and dust, respectively, generated in the process. The height and size of the features can be controlled by regulating the laser power (number of pulses per unit area) and laser beam aperture or use an appropriate milling cuter diameter. For finer features, the surface of the materials to be engraved must be coated with a high contrast surface layer. This enables the underlying substrate material to be gradually exposed, thus resulting to high contrast engravings. The rate of removal of the laser-induced excavated material also affects the feature profile. For example, the laser patterning technique has been employed in the fabrication of microfluidic channels, machining of optical waveguides in silica, and designing grating structure in fibres.[126]

Eutectic bonding for terahertz reflective devices

Eutectic bonding is a technique employed to permanently bond devices and wafers through the use of intermediate metallic film layers. This has been employed in hermetic or wafer-level vacuum packaging and fabrication of heat sinks in packaged microelectromechanical systems (MEMS) and smart sensing devices.[127,128] Unlike other conventional bonding techniques such as fusion, anodic, solder, and adhesive bonding, eutectic binding allows for less stringent conditions such as low temperature, tolerance to surface topology and surface cleanliness. More so, tens of nanometres at the interface of the two materials undergo liquid phase formation and alloying that creates a permanent bond with high mechanical stability.[127]

A sufficient amount of heat and pressure are employed to enable a significant composition of two adjacent metallic layers, *e.g.*, Au and Cr, or Au and crystalline Si (c-Si) layers, to diffuse into each other and form an alloy. At eutectic temperature, the intermediate layer undergoes a solid-to-liquid phase transition that can flow around contact layers to enable perfect permanent boning. For Au and Si bonding, Si nanoparticles diffuse in to Au as heat increases to form intermediate Au/Si layer that melts when an appropriate composition of Au:Si of 81:19 at% is attained. The melting temperature or eutectic temperature (350-400 ºC) is far less than that of either Au (1064 ºC) and Si (1414 ºC).[129] The eutectic phase formation, liquid phase transition, and subsequent solidification allows for wide

area, strong bonding strength. However, large areas increase the probability of voids in the eutectic liquid flow and could lead to poor bonding strength. Based on this limitation, proper removal of SiO_2 passivation layer off c-Si (through RCA and HF pre-treatment) introduction of subsidiary layers of titanium (Ti), platinum (Pt), and SiO_2 to facilitate diffusion, using Au–Au bonding, introduction of moderate roughness on the surfaces, and employing an amorphous Si (a-Si) interlayer to ease diffusion have been proposed to reduce the micro-voids and increase bonding strength.[130] Generally, an appropriate pre-treatment, eutectic temperature, and tooling force calibration as well as heating and cooling rates are critical for strong bonding strength.

Reflective terahertz devices can thus be realized by employing eutectic bonding techniques. In this case, the desired Si material is bonded directly to the Au ground plane, prior to DRIE processes. In a previous work, Headland *et al*. have employed a technique involving SU-8 assisted bonding to combine high-resistivity c-Si to a Au ground plane.[85,108]. Herein, they highlighted the use of Au–Au eutectic bonding and Au–c-Si bonding to realize high-efficiency reflective terahertz devices with high mechanical stability. These techniques were used to realize Si dielectric resonator-based quarter and half wave plates.[95] A wide range of terahertz devices from reflect arrays to active beam forming devices can be fabricated with this facile approach.

Summary and Outlook

Dielectric materials have been the foundation of advances in micro- and nano-electronic devices. The quality of dielectrics in terms of permittivity, defect sites and traps, and electric field breakdown has dictated performance and reliability. Likewise, microwave device efficiency has relied on dielectrics as substrates or as resonators. Terahertz devices have been limited by a combination of low terahertz power and materials with relatively high absorption. Dielectric materials with appropriate selection can enable improved efficiency in devices to create functional devices.

This review provides a comprehensive overview of the choice of dielectrics for terahertz frequencies. Categorizing dielectrics into two key roles – as spacer dielectrics and as resonant dielectric volumes – allows us to define suitable fabrication approaches. For spacers, thin film dielectrics can be used as sheets or spin-coated in liquid phase and solidified. For resonators, thin or thick film dielectrics and bulk materials can be shaped by etching or machining techniques. Understanding dielectric options and handling limitations opens up opportunities to harness a wider range of properties in designs by researchers in terahertz technology.

As terahertz devices become mainstream, faster adoption and translation will be enabled by endeavouring to adhere to silicon processing technology as much as possible. Adopting materials

used in other applications and incorporating for terahertz devices can unlock new opportunities, such as using nano-imprint resist COC as ultra-low-loss terahertz dielectric. Using techniques such as photolithography, vacuum deposition, plasma etching, and wafer bonding will ease translation and technology scale-up. Here, silicon-based structures either as absorbers based on moderately-doped silicon or resonant and transmission structures with high-resistivity silicon can capitalize on extensive availability of techniques and equipment.

Dielectrics hold the key to efficient terahertz devices and the next category of actively-tuned, high-speed communication applications. Managing the trade-off between functionality, fabrication processability, dielectric properties, and absorption will hold the key to high-performance terahertz technology.

Acknowledgements

The authors acknowledge collaborators and colleagues who have contributed to our published work included in this review. We acknowledge support of the Micro Nano Research Facility at RMIT University in the Victorian Node of the Australian National Fabrication Facility (ANFF). RTA and AU acknowledge support from the RMIT Research Stipend Scholarship and RMIT Research International Tuition Fee scholarship. We acknowledge project funding from the Australian Research Council through DP170101922 and equipment funding through LE120100004 and LE150100001.

References

[1] X. C. Zhang, A. Shkurinov, Y. Zhang, *Nature Photonics* 2017, 11, 16.
[2] T. Nagatsuma, G. Ducournau, C. C. Renaud, *Nature Photonics* 2016, 10, 371.
[3] H. Song, T. Nagatsuma, *IEEE Transactions on Terahertz Science and Technology* 2011, 1, 256.
[4] T. Kleine-Ostmann, T. Nagatsuma, *Journal of Infrared, Millimeter, and Terahertz Waves* 2011, 32, 143.
[5] K. B. Cooper, R. J. Dengler, N. Llombart, T. Bryllert, G. Chattopadhyay, E. Schlecht, J. Gill, C. Lee, A. Skalare, I. Mehdi, P. H. Siegel, *IEEE Transactions on Microwave Theory and Techniques* 2008, 56, 2771.
[6] K. B. Cooper, R. J. Dengler, G. Chattopadhyay, E. Schlecht, J. Gill, A. Skalare, I. Mehdi, P. H. Siegel, *IEEE Microwave and Wireless Components Letters* 2008, 18, 64.
[7] J. P. Guillet, B. Recur, L. Frederique, B. Bousquet, L. Canioni, I. Manek-Hönninger, P. Desbarats, P. Mounaix, *Journal of Infrared, Millimeter, and Terahertz Waves* 2014, 35, 382.
[8] P. U. Jepsen, D. G. Cooke, M. Koch, *Laser & Photonics Reviews* 2011, 5, 124.
[9] R. Appleby, H. B. Wallace, *IEEE Transactions on Antennas and Propagation* 2007, 55, 2944.
[10] H. Liu, H. Zhong, N. Karpowicz, Y. Chen, X. Zhang, *Proceedings of the IEEE* 2007, 95, 1514.
[11] F. M. Al-Douseri, Y. Chen, X.-C. Zhang, *International Journal of Infrared and Millimeter Waves* 2006, 27, 481.
[12] Q. Miao, L. Tian, K. Zhao, Q. Zhou, Y. Shi, D. Zhao, S. Zhao, C. Zhang, *Journal of Physics: Conference Series* 2011, 276, 012220.

[13] E. Philip, M. Zeki Güngördü, S. Pal, P. Kung, S. M. Kim, *Journal of Infrared, Millimeter, and Terahertz Waves* 2017, 38, 1047.
[14] J.-H. Son, *Journal of Applied Physics* 2009, 105, 102033.
[15] M. Walther, P. Plochocka, B. Fischer, H. Helm, P. Uhd Jepsen, *Biopolymers* 2002, 67, 310.
[16] O. A. Smolyanskaya, N. V. Chernomyrdin, A. A. Konovko, K. I. Zaytsev, I. A. Ozheredov, O. P. Cherkasova, M. M. Nazarov, J. P. Guillet, S. A. Kozlov, Y. V. Kistenev, J. L. Coutaz, P. Mounaix, V. L. Vaks, J. H. Son, H. Cheon, V. P. Wallace, Y. Feldman, I. Popov, A. N. Yaroslavsky, A. P. Shkurinov, V. V. Tuchin, *Progress in Quantum Electronics* 2018, 62, 1.
[17] B. Ferguson, X.-C. Zhang, *Nature Materials* 2002, 1, 26.
[18] W. Withayachumnankul, D. Abbott, *IEEE Photonics Journal* 2009, 1, 99.
[19] N. I. Zheludev, Y. S. Kivshar, *Nature Materials* 2012, 11, 917.
[20] C. M. Watts, X. Liu, W. J. Padilla, *Advanced Materials* 2012, 24, OP98.
[21] I. Al-Naib, W. Withayachumnankul, *Journal of Infrared, Millimeter, and Terahertz Waves* 2017, 38, 1067.
[22] J. He, Y. Zhang, *Journal of Physics D: Applied Physics* 2017, 50, 464004.
[23] A. F. J. Levi, in *Essential Classical Mechanics for Device Physics*, Morgan & Claypool Publishers, 2016, 6.
[24] in *Encyclopedia of RF and Microwave Engineering*.
[25] P. Genevet, F. Capasso, F. Aieta, M. Khorasaninejad, R. Devlin, *Optica* 2017, 4, 139.
[26] Q. He, S. Sun, S. Xiao, L. Zhou, *Advanced Optical Materials* 2018, 6, 1800415.
[27] V.-C. Su, C. H. Chu, G. Sun, D. P. Tsai, *Opt. Express* 2018, 26, 13148.
[28] S. K. K. Dash, T. Khan, Y. M. M. Antar, *International Journal of RF and Microwave Computer-Aided Engineering* 2018, 28, e21270.
[29] S. Jahani, Z. Jacob, *Nature Nanotechnology* 2016, 11, 23.
[30] S. K. K. Dash, T. Khan, A. De, *International Journal of RF and Microwave Computer-Aided Engineering* 2017, 27, e21069.
[31] S. Qu, H. Yi, B. J. Chen, K. B. Ng, C. H. Chan, *Proceedings of the IEEE* 2017, 105, 1166.
[32] S. Walia, C. M. Shah, P. Gutruf, H. Nili, D. R. Chowdhury, W. Withayachumnankul, M. Bhaskaran, S. Sriram, *Applied Physics Reviews* 2015, 2, 011303.
[33] A. Ferraro, D. C. Zografopoulos, R. Caputo, R. Beccherelli, *IEEE Journal of Selected Topics in Quantum Electronics* 2017, 23, 1.
[34] Y. Wen, W. Ma, J. Bailey, G. Matmon, X. Yu, G. Aeppli, *Opt. Lett.* 2014, 39, 1589.
[35] C. Gong, M. Zhan, J. Yang, Z. Wang, H. Liu, Y. Zhao, W. Liu, *Scientific Reports* 2016, 6, 32466.
[36] T. Niu, W. Withayachumnankul, A. Upadhyay, P. Gutruf, D. Abbott, M. Bhaskaran, S. Sriram, C. Fumeaux, *Opt. Express* 2014, 22, 16148.
[37] A. Ferraro, D. C. Zografopoulos, M. Missori, M. Peccianti, R. Caputo, R. Beccherelli, *Opt. Lett.* 2016, 41, 2009.
[38] H.-T. Chen, W. J. Padilla, J. M. O. Zide, A. C. Gossard, A. J. Taylor, R. D. Averitt, *Nature* 2006, 444, 597.
[39] J. E. Heyes, W. Withayachumnankul, N. K. Grady, D. R. Chowdhury, A. K. Azad, H.-T. Chen, *Applied Physics Letters* 2014, 105, 181108.
[40] T. Niu, W. Withayachumnankul, B. S. Y. Ung, H. Menekse, M. Bhaskaran, S. Sriram, C. Fumeaux, *Opt. Express* 2013, 21, 2875.
[41] L. Cong, W. Cao, X. Zhang, Z. Tian, J. Gu, R. Singh, J. Han, W. Zhang, *Applied Physics Letters* 2013, 103, 171107.
[42] F. Pavanello, F. Garet, M.-B. Kuppam, E. Peytavit, M. Vanwolleghem, F. Vaurette, J.-L. Coutaz, J.-F. Lampin, *Applied Physics Letters* 2013, 102, 111114.
[43] A. Ebrahimi, S. Nirantar, W. Withayachumnankul, M. Bhaskaran, S. Sriram, S. F. Al-Sarawi, D. Abbott, *IEEE Transactions on Terahertz Science and Technology* 2015, 5, 761.
[44] T. Niu, A. Upadhyay, W. Withayachumnankul, D. Headland, D. Abbott, M. Bhaskaran, S. Sriram, C. Fumeaux, *Applied Physics Letters* 2015, 107, 031111.

[45] N. K. Grady, J. E. Heyes, D. R. Chowdhury, Y. Zeng, M. T. Reiten, A. K. Azad, A. J. Taylor, D. A. R. Dalvit, H.-T. Chen, *Science* 2013, 340, 1304.
[46] M. Jia, Z. Wang, H. Li, X. Wang, W. Luo, S. Sun, Y. Zhang, Q. He, L. Zhou, *Light: Science & Applications* 2019, 8, 16.
[47] Q. Li, L. Cong, R. Singh, N. Xu, W. Cao, X. Zhang, Z. Tian, L. Du, J. Han, W. Zhang, *Nanoscale* 2016, 8, 17278.
[48] D. Headland, T. Niu, E. Carrasco, D. Abbott, S. Sriram, M. Bhaskaran, C. Fumeaux, W. Withayachumnankul, *IEEE Journal of Selected Topics in Quantum Electronics* 2017, 23, 1.
[49] L. Cong, Y. K. Srivastava, H. Zhang, X. Zhang, J. Han, R. Singh, *Light: Science & Applications* 2018, 7, 28.
[50] Y. Harada, M. S. Ukhtary, M. Wang, S. K. Srinivasan, E. H. Hasdeo, A. R. T. Nugraha, G. T. Noe, Y. Sakai, R. Vajtai, P. M. Ajayan, R. Saito, J. Kono, *ACS Photonics* 2017, 4, 121.
[51] S. Arezoomandan, H. Condori Quispe, A. Chanana, P. Gopalan, S. Banerji, A. Nahata, B. Sensale-Rodriguez, *Semiconductor Science and Technology* 2018, 33, 104007.
[52] R. Singh, W. Cao, I. Al-Naib, L. Cong, W. Withayachumnankul, W. Zhang, *Applied Physics Letters* 2014, 105, 171101.
[53] Y. Z. Cheng, W. Withayachumnankul, A. Upadhyay, D. Headland, Y. Nie, R. Z. Gong, M. Bhaskaran, S. Sriram, D. Abbott, *Applied Physics Letters* 2014, 105, 181111.
[54] S. Ma, X. Wang, W. Luo, S. Sun, Y. Zhang, Q. He, L. Zhou, *EPL (Europhysics Letters)* 2017, 117, 37007.
[55] Y. Zheng, Y. Zhou, J. Gao, X. Cao, H. Yang, S. Li, L. Xu, J. Lan, L. Jidi, *Scientific Reports* 2017, 7, 16137.
[56] S. A. Baig, J. L. Boland, D. A. Damry, H. H. Tan, C. Jagadish, H. J. Joyce, M. B. Johnston, *Nano Letters* 2017, 17, 2603.
[57] F. Pavanello, G. Ducournau, E. Peytavit, S. Lepilliet, J. F. Lampin, *IEEE Antennas and Wireless Propagation Letters* 2014, 13, 939.
[58] P. D. Cunningham, N. N. Valdes, F. A. Vallejo, L. M. Hayden, B. Polishak, X.-H. Zhou, J. Luo, A. K. Y. Jen, J. C. Williams, R. J. Twieg, *Journal of Applied Physics* 2011, 109, 043505.
[59] D. Headland, P. Thurgood, D. Stavrevski, W. Withayachumnankul, D. Abbott, M. Bhaskaran, S. Sriram, *Opt. Mater. Express* 2015, 5, 1373.
[60] A. J. Gatesman, J. Waldman, M. Ji, C. Musante, S. Yagvesson, *IEEE Microwave and Guided Wave Letters* 2000, 10, 264.
[61] E. Perret, N. Zerounian, S. David, F. Aniel, *Microelectronic Engineering* 2008, 85, 2276.
[62] E. Motaharifar, R. G. Pierce, R. Islam, R. Henderson, J. W. P. Hsu, M. Lee, *Journal of Infrared, Millimeter, and Terahertz Waves* 2018, 39, 93.
[63] T. Driscoll, G. O. Andreev, D. N. Basov, S. Palit, S. Y. Cho, N. M. Jokerst, D. R. Smith, *Applied Physics Letters* 2007, 91, 062511.
[64] H. Chu, Y. Guo, T. Lim, Y. M. Khoo, X. Shi, *IEEE Transactions on Antennas and Propagation* 2012, 60, 4582.
[65] J. T. Beechinor, E. McGlynn, M. O'Reilly, G. M. Crean, *Microelectronic Engineering* 1997, 33, 363.
[66] N. Ivanović, N. Marjanović, Z. Rakočević, V. Andrić, B. Hadžić, I. Vukanac, I. Durdević, M. Srećković, *Progress in Organic Coatings* 2013, 76, 257.
[67] P. Nunes, P. Ohlsson, O. O. Sala, J. P. Kutter, *Microfluidics and Nanofluidics* 2010, 9, 145.
[68] I. Maestrojuan, I. Palacios, I. Ederra, R. Gonzalo, *Microwave and Optical Technology Letters* 2015, 57, 371.
[69] E. Peytavit, C. Donche, S. Lepilliet, G. Ducournau, J. F. Lampin, *Electronics Letters* 2011, 47, 453.
[70] K. Nielsen, H. K. Rasmussen, A. J. L. Adam, P. C. M. Planken, O. Bang, P. U. Jepsen, *Opt. Express* 2009, 17, 8592.
[71] P. S. Nunes, P. D. Ohlsson, O. Ordeig, J. P. Kutter, *Microfluidics and Nanofluidics* 2010, 9, 145.

[72] D. Nikolova, E. Dayss, G. Leps, A. Wutzler, *Surface and Interface Analysis* 2004, 36, 689.
[73] S.-J. Hwang, M.-C. Tseng, J.-R. Shu, H. Her Yu, *Surface and Coatings Technology* 2008, 202, 3669.
[74] N. Keller, T. M. Nargang, M. Runck, F. Kotz, A. Striegel, K. Sachsenheimer, D. Klemm, K. Länge, M. Worgull, C. Richter, *Lab on a Chip* 2016, 16, 1561.
[75] Q. Tang, M. Liang, Y. Lu, P. K. Wong, G. J. Wilmink, H. Xin, *Development of terahertz (THz) microfluidic devices for "Lab-on-a-Chip" applications*, Vol. 8585, SPIE, 2013.
[76] C. Chou, M.-H. Yang, *Journal of Thermal Analysis* 1993, 40, 657.
[77] T. Dollase, H. W. Spiess, M. Gottlieb, R. Yerushalmi-Rozen, *Europhysics Letters (EPL)* 2002, 60, 390.
[78] J. A. Hejase, P. R. Paladhi, P. Chahal, "Terahertz packaging: Study of substrates for novel component designs", presented at *2010 Proceedings 60th Electronic Components and Technology Conference (ECTC)*, 1-4 June 2010, 2010.
[79] S. Dabral, J. Van Etten, X. Zhang, C. Apblett, G. R. Yang, P. Ficalora, J. F. McDonald, *Journal of Electronic Materials* 1992, 21, 989.
[80] PARA-TECH-COATING, *Parylene datasheet (http://www.parylene.com/pdfs/PTC-Parylene_Properties_Chart.pdf)* 2019.
[81] L. M. Diaz-Albarran, E. Lugo-Hernandez, E. Ramirez-Garcia, M. A. Enciso-Aguilar, D. Valdez-Perez, P. Cereceda-Company, D. Granados, J. L. Costa-Krämer, *Microelectronic Engineering* 2018, 191, 84.
[82] R. A. Kirchhoff, C. J. Carriere, K. J. Bruza, N. G. Rondan, R. L. Sammler, *Journal of Macromolecular Science: Part A - Chemistry* 1991, 28, 1079.
[83] H. Chen, J. Wang, H. Ma, S. Qu, Z. Xu, A. Zhang, M. Yan, Y. Li, *Journal of Applied Physics* 2014, 115, 154504.
[84] R. D. Richtmyer, *Journal of Applied Physics* 1939, 10, 391.
[85] D. Headland, S. Nirantar, W. Withayachumnankul, P. Gutruf, D. Abbott, M. Bhaskaran, C. Fumeaux, S. Sriram, *Advanced Materials* 2015, 27, 7137.
[86] D. Headland, E. Carrasco, S. Nirantar, W. Withayachumnankul, P. Gutruf, J. Schwarz, D. Abbott, M. Bhaskaran, S. Sriram, J. Perruisseau-Carrier, C. Fumeaux, *ACS Photonics* 2016, 3, 1019.
[87] Z. Ma, S. M. Hanham, P. Albella, B. Ng, H. T. Lu, Y. Gong, S. A. Maier, M. Hong, *ACS Photonics* 2016, 3, 1010.
[88] X. Jiang, H. Chen, Z. Li, H. Yuan, L. Cao, Z. Luo, K. Zhang, Z. Zhang, Z. Wen, L.-g. Zhu, X. Zhou, G. Liang, D. Ruan, L. Du, L. Wang, G. Chen, *Opt. Express* 2018, 26, 14132.
[89] H. Zhang, X. Zhang, Q. Xu, Q. Wang, Y. Xu, M. Wei, Y. Li, J. Gu, Z. Tian, C. Ouyang, X. Zhang, C. Hu, J. Han, W. Zhang, *Photon. Res.* 2018, 6, 24.
[90] H. Zhang, X. Zhang, Q. Xu, C. Tian, Q. Wang, Y. Xu, Y. Li, J. Gu, Z. Tian, C. Ouyang, X. Zhang, C. Hu, J. Han, W. Zhang, *Advanced Optical Materials* 2018, 6, 1700773.
[91] D. Jia, Y. Tian, W. Ma, X. Gong, J. Yu, G. Zhao, X. Yu, *Opt. Lett.* 2017, 42, 4494.
[92] D. Jia, Y. Tian, W. Ma, X. Gong, J. Yu, G. Zhao, X. Yu, "Dielectric gradient metasurface for efficient terahertz wave focusing", presented at *2018 IEEE Micro Electro Mechanical Systems (MEMS)*, 21-25 Jan. 2018, 2018.
[93] W. S. L. Lee, K. Kaltenecker, S. Nirantar, W. Withayachumnankul, M. Walther, M. Bhaskaran, B. M. Fischer, S. Sriram, C. Fumeaux, *Opt. Express* 2017, 25, 3756.
[94] Q. Yu, J. Gu, Q. Yang, Y. Zhang, Y. Li, Z. Tian, C. Ouyang, J. Han, J. F. O. Hara, W. Zhang, *IEEE Photonics Journal* 2017, 9, 1.
[95] W. S. L. Lee, R. T. Ako, M. X. Low, M. Bhaskaran, S. Sriram, C. Fumeaux, W. Withayachumnankul, *Opt. Express* 2018, 26, 14392.
[96] M. Chen, F. Fan, S.-T. Xu, S.-J. Chang, *Scientific Reports* 2016, 6, 38562.
[97] J. Zi, Q. Xu, Q. Wang, C. Tian, Y. Li, X. Zhang, J. Han, W. Zhang, *Applied Physics Letters* 2018, 113, 101104.
[98] X.-P. Dong, J.-R. Cheng, F. Fan, S.-T. Xu, X.-H. Wang, S.-J. Chang, *Opt. Express* 2019, 27, 202.

[99] W. Withayachumnankul, C. M. Shah, C. Fumeaux, K. Kaltenecker, M. Walther, B. M. Fischer, D. Abbott, M. Bhaskaran, S. Sriram, *Advanced Optical Materials* 2013, 1, 443.
[100] W. Withayachumnankul, C. M. Shah, C. Fumeaux, B. S. Y. Ung, W. J. Padilla, M. Bhaskaran, D. Abbott, S. Sriram, *ACS Photonics* 2014, 1, 625.
[101] S. Yin, J. Zhu, W. Xu, W. Jiang, J. Yuan, G. Yin, L. Xie, Y. Ying, Y. Ma, *Applied Physics Letters* 2015, 107, 073903.
[102] K. Fan, J. Y. Suen, X. Liu, W. J. Padilla, *Optica* 2017, 4, 601.
[103] Y. Z. Cheng, W. Withayachumnankul, A. Upadhyay, D. Headland, Y. Nie, R. Z. Gong, M. Bhaskaran, S. Sriram, D. Abbott, *Advanced Optical Materials* 2015, 3, 376.
[104] S. M. Hanham, A. I. Fernández-Domínguez, J. H. Teng, S. S. Ang, K. P. Lim, S. F. Yoon, C. Y. Ngo, N. Klein, J. B. Pendry, S. A. Maier, *Advanced Materials* 2012, 24, OP226.
[105] L.-H. Du, J. Li, Z.-H. Zhai, K. Meng, Q. Liu, S.-C. Zhong, P.-W. Zhou, L.-G. Zhu, Z.-R. Li, Q.-X. Peng, *AIP Advances* 2016, 6, 055112.
[106] K. Fan, J. Zhang, X. Liu, G.-F. Zhang, R. D. Averitt, W. J. Padilla, *Advanced Materials* 2018, 30, 1800278.
[107] X. Zhao, Y. Wang, J. Schalch, G. Duan, K. Cremin, J. Zhang, C. Chen, R. D. Averitt, X. Zhang, *ACS Photonics* 2019, 6, 830.
[108] D. Headland, W. Withayachumnankul, S. Nirantary, M. Bhaskarany, S. Sriramy, C. Fumeaux, "High-efficiency dielectric resonator antennas in the terahertz range", presented at *2016 IEEE MTT-S International Microwave Workshop Series on Advanced Materials and Processes for RF and THz Applications (IMWS-AMP)*, 20-22 July 2016, 2016.
[109] M. H. Jamaluddin, R. Sauleau, X. Castel, R. Benzerga, L. L. Coq, R. Gillard, T. Koleck, *Progress In Electromagnetics Research B* 2010, 25, 261.
[110] U. Chakraborty, A. K. Biswas, S. Maity, B. Roy, S. Roy, *International Journal of RF and Microwave Computer-Aided Engineering* 2019, 29, e21529.
[111] L. Zou, W. Withayachumnankul, C. M. Shah, A. Mitchell, M. Bhaskaran, S. Sriram, C. Fumeaux, *Opt. Express* 2013, 21, 1344.
[112] L. Zou, M. López-García, W. Withayachumnankul, C. M. Shah, A. Mitchell, M. Bhaskaran, S. Sriram, R. Oulton, M. Klemm, C. Fumeaux, *Applied Physics Letters* 2014, 105, 191109.
[113] S. Sun, Z. Zhou, C. Zhang, W. Yang, Q. Song, S. Xiao, *Annalen der Physik* 2018, 530, 1700418.
[114] D. Headland, Y. Monnai, D. Abbott, C. Fumeaux, W. Withayachumnankul, *APL Photonics* 2018, 3, 051101.
[115] R. Yahiaoui, K. Hanai, K. Takano, T. Nishida, F. Miyamaru, M. Nakajima, M. Hangyo, *Opt. Lett.* 2015, 40, 3197.
[116] A. Berrier, P. Albella, M. A. Poyli, R. Ulbricht, M. Bonn, J. Aizpurua, J. G. Rivas, *Opt. Express* 2012, 20, 5052.
[117] X. Zhao, Y. Wang, J. Schalch, G. Duan, K. Cremin, J. Zhang, C. Chen, R. D. Averitt, X. Zhang, *ACS Photonics* 2019.
[118] M. B. Johnston, "THz modulators and detectors based on semiconductor nanowires", presented at *2017 42nd International Conference on Infrared, Millimeter, and Terahertz Waves (IRMMW-THz)*, 27 Aug.-1 Sept. 2017, 2017.
[119] B. Sensale-Rodriguez, R. Yan, M. M. Kelly, T. Fang, K. Tahy, W. S. Hwang, D. Jena, L. Liu, H. G. Xing, *Nature Communications* 2012, 3, 780.
[120] C. J. Docherty, S. D. Stranks, S. N. Habisreutinger, H. J. Joyce, L. M. Herz, R. J. Nicholas, M. B. Johnston, *Journal of Applied Physics* 2014, 115, 203108.
[121] Y. Liu, T. Zhu, J. Feng, S. Yuan, X. Zhao, T. Wu, H. Zeng, *Opt. Express* 2018, 26, 17025.
[122] R. Wang, L. Xie, S. Hameed, C. Wang, Y. Ying, *Carbon* 2018, 132, 42.
[123] C. Lan, D. Zhu, J. Gao, B. Li, Z. Gao, *Opt. Express* 2018, 26, 11633.
[124] A. Berrier, R. Ulbricht, M. Bonn, J. G. Rivas, *Opt. Express* 2010, 18, 23226.
[125] L. Deng, J. Teng, H. Liu, Q. Y. Wu, J. Tang, X. Zhang, S. A. Maier, K. P. Lim, C. Y. Ngo, S. F. Yoon, S. J. Chua, *Advanced Optical Materials* 2013, 1, 128.

[126] L. Minkevičius, S. Indrišiūnas, R. Šniaukas, B. Voisiat, V. Janonis, V. Tamošiūnas, I. Kašalynas, G. Račiukaitis, G. Valušis, *Opt. Lett.* 2017, 42, 1875.
[127] A. Hilton, D. S. Temple, *Sensors (Basel, Switzerland)* 2016, 16, 1819.
[128] D. D. E. Jr., Z. Bok, *International Symposium on Microelectronics* 2010, 2010, 000898.
[129] Y. Lin, M. Baum, M. Haubold, J. Fromel, M. Wiemer, T. Gessner, M. Esashi, "Development and evaluation of AuSi eutectic wafer bonding", presented at *TRANSDUCERS 2009 - 2009 International Solid-State Sensors, Actuators and Microsystems Conference*, 21-25 June 2009, 2009.
[130] M. Abouie, Q. Liu, D. G. Ivey, *Materials Science and Engineering: B* 2012, 177, 1748.